

## Supplemental data

**Supplemental Figure 1. Co-staining of CD3 with IL-17 or IL-22 in colon mucosal specimens from HIV-negative and HIV-1-positive subjects by confocal microscopy (at 400 ×).** Representative staining shows CD3<sup>+</sup> (green), IL-17<sup>+</sup> or IL-22<sup>+</sup> (red) cells. DAPI was used to counterstain nuclear DNA (blue).

**Supplemental Figure 2. Gating strategy of human ILC3s in leukocytes from lymphoid organs of humanized mice.** Flow cytometry of viable (Y7<sup>-</sup>) human splenocytes (mCD45<sup>-</sup>hCD45<sup>+</sup>) stained for lineages<sup>-</sup> (CD3, CD14, CD16, CD19, CD20, CD11c, CD123, CD34) and for CD127<sup>+</sup>CD117<sup>+</sup> ILC3s. Human NKp44<sup>+</sup> (NCR<sup>+</sup>) and NKp44<sup>-</sup> (NCR<sup>-</sup>) ILC3s subsets are both detected in humanized mice.

**Supplemental Figure 3. Splenic ILC3s from humanized mice (n = 4) have similar potentials to produce IL-17a and IL-22 as human peripheral ILC3s (n = 6) in response to IL-1β and IL-23 *in vitro*.** Representative FACS plots show the percentages of IL-17a- and IL-22-producing ILC3s in response to medium, IL-12 (20 ng/ml) plus IL-18 (20 ng/ml), IL-1β(20 ng/ml) plus IL-23 (20 ng/ml) and PMA plus ionomycin.

**Supplemental Figure 4. Persistent HIV-1 infection has similar effect on the relative frequency of NCR<sup>+</sup> and NCR<sup>-</sup> ILC3 subsets from BM, mLN and spleen of humanized mice.** Mock, n = 12; HIV-1-infected, n = 6; HIV-1-infected and cART-treated NRG-hu mice, n = 8.

**Supplemental Figure 5. Correlation analysis of ILC3 percentage and pDC frequency in mLN of humanized mice (Spearman rank correlation test).** *r*, correlation coefficients, and *P* values are shown.

**Supplemental Figure 6. Depletion of pDCs doesn't influence the ILC3 percentage**

**in mock control humanized mice (n = 3).** Representative FACS plots show the percentages of ILC3s in pLN (peripheral lymph node), spleen and mLN (mesenteric lymph node) from mock humanized mice with or without pDC depletion. Numbers indicate percentages of ILC3s.

**Supplemental Figure 7. HIV-1 infection-induced IFN- $\alpha$  production depends on pDCs in splenocytes cultured *ex vivo*.** Splenocytes from humanized mice were infected with mock or HIV-1 in the absence or presence of 15B-SAP (pDC immune-toxin, 8 ng/ml), or CpG-A (10  $\mu$ g/ml) for 3 days. The supernatants were collected and analyzed for IFN- $\alpha$  concentration by ELISA. \*\*\* $P < 0.001$ , one-way ANOVA with Tukey post-hoc test.

**Supplementary Table 1. Characteristics of subjects enrolled in the study**

Groups	Healthy controls (HC)	HIV CD4 > 400 cells/ $\mu$ l	HIV CD4 < 400 cells/ $\mu$ l
Cases	20	18	37
Age (year)	32 (19-54)	36 (21-55)	34 (18-53)
Sex (m/f)	19/1	17/1	35/2
CD4 counts (cells/ $\mu$ l)	NA	547 (402-986)	327 (9-386)
HIV-1 loads (copies/ml)	NA	36, 540 (<40-299,000)	76, 900 (4000-582,000)
Infection route (s/b/nd)*	NA	16/0/2	27/2/8

NA, not applicable; Data are median (range). \* b/s, b blood; s, sex; nd, not determined

**Supplementary Table 2. Flurochrome-conjugated antibodies used in the study**

<b>Flurochrome</b>	<b>Antibody</b>	<b>Company</b>	<b>Clone #</b>	<b>Cat #</b>
FITC	Anti-human CD69	BioLegend	FN50	310904
Alexa Fluor488	Anti-human RORgt	BD Bioscience	Q21-559	563621
Alexa Fluor488	Anti-human GrB	BD Bioscience	GB11	561998
FITC	Anti-human CCR5	BD Bioscience	2D7/CCR5	555992
FITC	Anti-human CD45RA	BioLegend	HI100	304106
FITC	Anti-human CD94	BioLegend	DX22	305504
FITC	Anti-human CD103	BioLegend	Ber-ALT8	350204
FITC	Anti-human CD8a	BioLegend	RPA-T8	301006
FITC	Anti-human IL-17a	eBioscience	EBio64DEL17	11-7179-42
FITC	Anti-human IFN- $\gamma$	BioLegend	4S.B3	502506
FITC	Anti-human Ki67	BD Bioscience	B56	556026
FITC	Anti-human IL-1R1	R&D System		FAB269F
FITC	Anti-BrdU	eBioscience	Bu20a	11-5071-41
FITC	KC57 (P24)	Coulter Clone		6604665
PE	Anti-human T-bet	BioLegend	4B10	644809
PE	Anti-human GATA3	BioLegend	16E10A23	653803
PE	Anti-human CXCR4	BD Bioscience	12G5	555974
PE	Anti-human CCR6	BioLegend	G034E3	353409
PE	Anti-human CD161	BioLegend	HP-3G10	339904
PE	Anti-human CD25	BioLegend	BC96	302606
PE	Anti-human NKp46	BioLegend	9E2	331908
PE	Anti-human CD11a	BioLegend	HI111	301207
PE	Anti-human NKp44	BioLegend	P44-8	325108
PE	Anti-human IL-13	BioLegend	JES10-5A2	501903
PE	Anti-human IL-22	eBioscience	22URTI	12-7229-42
PE	Active Rabbit anti-caspase-3	BD Bioscience	C92-605	550914
PE-TR	Anti-human CD4	Invitrogen	S3.5	MHCD0417
PE-TR	Anti-human CD56	Invitrogen	MEM-188	MHCD5617
PE-TR	Anti-human CD38	Invitrogen	HIT2	MHCD3817
PE-TR	Anti-human CD8	Invitrogen	3B5	MHCD0817
PE-TR	Anti-human CD3	Invitrogen	S4.1	MHCD0317
PE-Cy5	Anti-human CD3	BioLegend	HIT3a	300310
TRI-COLOR	Anti-human CD14	Invitrogen	TÜK4	MHCD1406
PE-Cy5	Anti-human CD16	BioLegend	3G8	302010
PE-Cy5	Anti-human CD19	BioLegend	HIB19	302210
PE-Cy5	Anti-human CD20	BioLegend	2H7	302308
PE-Cy5	Anti-human CD11c	BioLegend	3.9	301610
PE-Cy5	Anti-human CD123	BioLegend	6H6	306008
PE-Cy5	Anti-human CD34	BD Bioscience	581	555823
PE-Cy7	Anti-human CD117	BioLegend	104D2	313212
Brilliant Violet 421	Anti-human CD127	BioLegend	A019D5	351310
Yellow fluorescent	reactive dye (Y7)	Life Tech		L34959

Pacific Orange	Anti-mouse CD45	Life Tech	30-F11	MCD4530
AF647	Anti-human CRTH2	BioLegend	BM16	350104
APC	NKp44	BioLegend	P44-8	325110
APC-Cy7	Anti-human CD45	BioLegend	HI30	304014

---

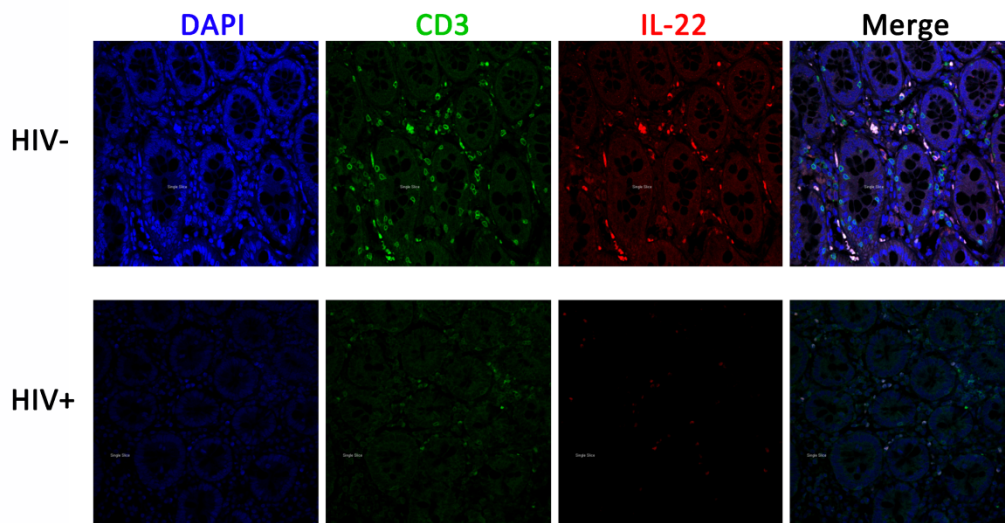
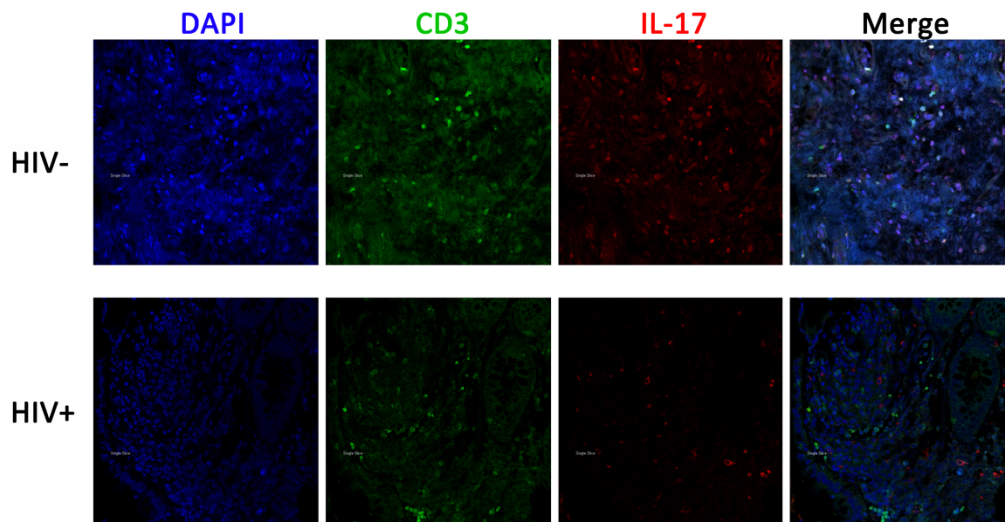
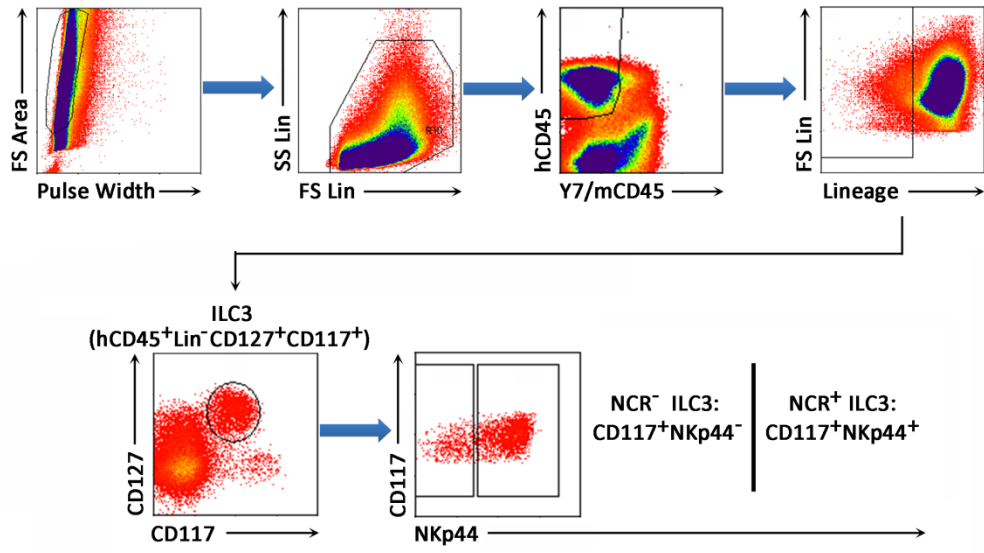
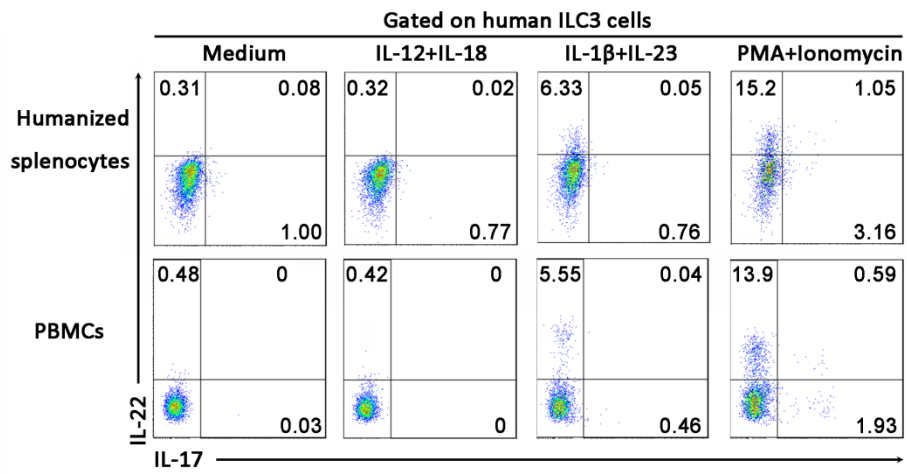


Figure S1



**Figure S2**



**Figure S3**

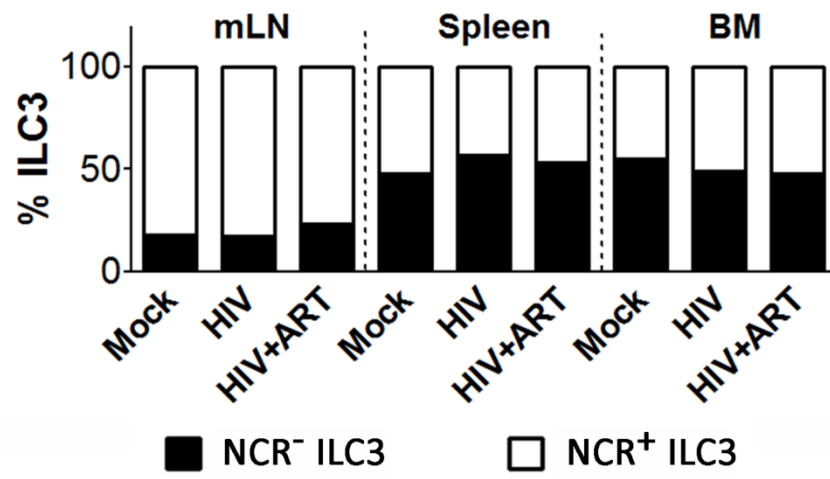


Figure S4

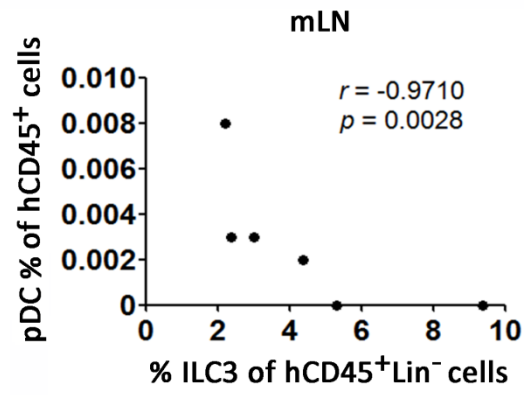
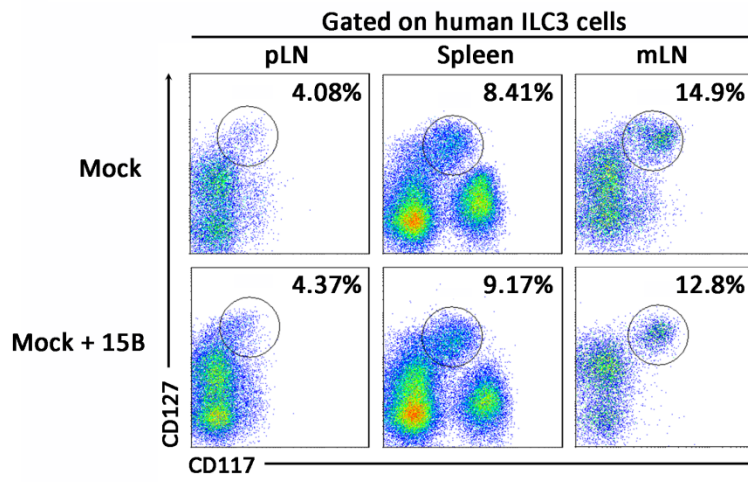


Figure S5



**Figure S6**

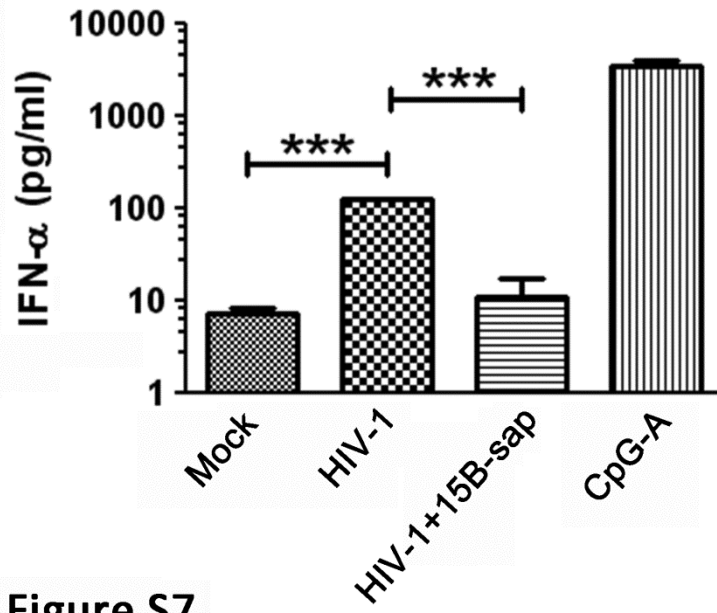


Figure S7